I&EC research
Industrial & Engineering Chemistry Research

pubs.acs.org/IECR

Article

Sulfonated Phenol–Formaldehyde Resins for Highly Efficient, Selective, and Reversible Adsorption of NH_3

Chen Tan, Zhang-Min Li,* Ming-Shuai Sun, Hua Guan, Yan Zhou,* and Duan-Jian Tao

Cite This: *Ind. Eng. Chem. Res.* 2023, 62, 1542−1549

Read Online

ACCESS | Metrics & More | Article Recommendations | Supporting Information

ABSTRACT: Currently available liquid absorbents and porous adsorbents for capturing NH_3 are often unfavorable in terms of possessing high stability and reusability. Herein, three novel sulfonated phenol–formaldehyde (SPF) resins with almost non-porosity were prepared through a facile polymerization of various phenol sulfonates with formaldehyde and applied to the adsorption of NH_3. It is demonstrated that the SPF–Na resin displayed excellent reversibility and good stability for efficient NH_3 adsorption (12.87 mmol·g^{-1}) and superior ideal adsorption solution theory selectivities for 3% NH_3/97% N_2 (5076) and 3% NH_3/97% H_2 (2619) at 298.2 K and 1.0 bar even in 20 adsorption–desorption cycles, whereas common PF resin only achieved a very low capacity of 1.9 mmol·g^{-1}. Column breakthrough results further confirmed that the SPF–Na resin showed good performance in selective adsorption of 3% NH_3 in the mixture of $NH_3/N_2/H_2$. Nonporous SPF resins with high stability, desired capacity, and outstanding reversibility are perceived as promising solid adsorbents for effectively capturing NH_3 in the ammonia industry.

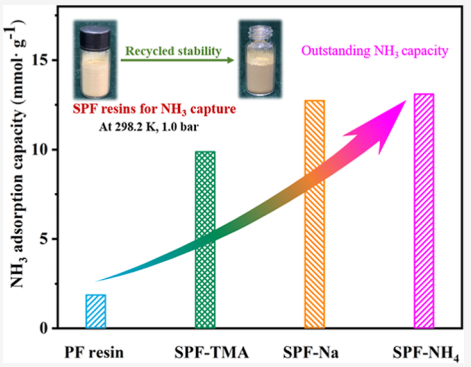

INTRODUCTION

Ammonia (NH_3), as an irreplaceable raw material in our daily lives, especially for the agriculture and industry, is widely used for the synthesis of fertilizers, pharmaceutical products, and many nitrogen-containing inorganic salts and organic intermediates.[1−3] With the help of a popular freezing method, NH_3 can be mostly separated from H_2 and N_2, but the tail gas containing a low concentration of NH_3 is hard to be recycled efficiently. Besides, NH_3 is a toxic, corrosive, and reactive gas giving rise to the problems of industrial safety and the environment. For example, NH_3 in the air would combine with SO_2 and NO_x to form PM 2.5, which is a severe menace to public security.[4−7] Thus, it is an important task for effective and reversible adsorption of low-concentration NH_3, which needs adsorbents possessing abilities to quickly capture NH_3 and release it reversibly.

To this demand, many endeavors have been focused on exploring efficient solid adsorbents, such as zeolites,[8] mesoporous silica,[9] activated carbons,[10] porous dyes,[11] covalent organic frameworks (COFs),[12] porous polymers,[13] and metal–organic frameworks (MOFs),[14−16] to capture toxic NH_3. However, the synthesis of most of these materials is tedious, or the raw materials are difficult to obtain. In addition, harsh conditions including the higher temperature and longer time for regeneration of these materials would lead to a serious collapse of their porous structure, as illustrated in Scheme 1.[17−20] As a result, the reused adsorbent materials mentioned above usually have a decrease in adsorption capacity and selectivity of NH_3 after several recycles.

Recently, various phenol-based liquid absorbents were widely reported for efficient absorption of NH_3.[21−23] NH_3 can be captured by utilizing the acidity of the phenolic hydroxyl group. However, it is seen from Scheme 1 that a fresh phenol-based deep eutectic solvent is easily oxidized in air and turns from colorless to purple, showing that phenol-based deep eutectic solvents are not stable enough. By contrast, phenol–formaldehyde (PF) resin as a common polymer is popularly used in many industries owing to its unique properties including heat resistance and excellent mechanical stability.[24,25] Bandosz et al. reported that a kind of resorcinol-based PF resins could be employed for adsorption of NH_3.[26] However, the uptake capacity of NH_3 was too low (<2.0 mmol/g), and the NH_3 adsorption process is even irreversible. Given the basicity of NH_3, it is possible that doping acidic sites into PF resin would achieve highly efficient and selective adsorption of NH_3. As is well-known, sulfonated phenol–formaldehyde (SPF) resin has a molecular structure similar to that of PF resin, which is synthesized from formaldehyde and 4-hydroxybenzenesulfonic acid.[27] The resulting SPF resin has a high density of sulfonate groups, which can show a strong interaction with NH_3. Considering the inadequate research on

Received: October 19, 2022
Revised: December 15, 2022
Accepted: December 30, 2022
Published: January 10, 2023

https://doi.org/10.1021/acs.iecr.2c03789
Ind. Eng. Chem. Res. 2023, 62, 1542−1549

Scheme 1. Comparison of NH_3 Capture by Porous Materials, Liquid Absorbents, and SPF Resin Adsorbents

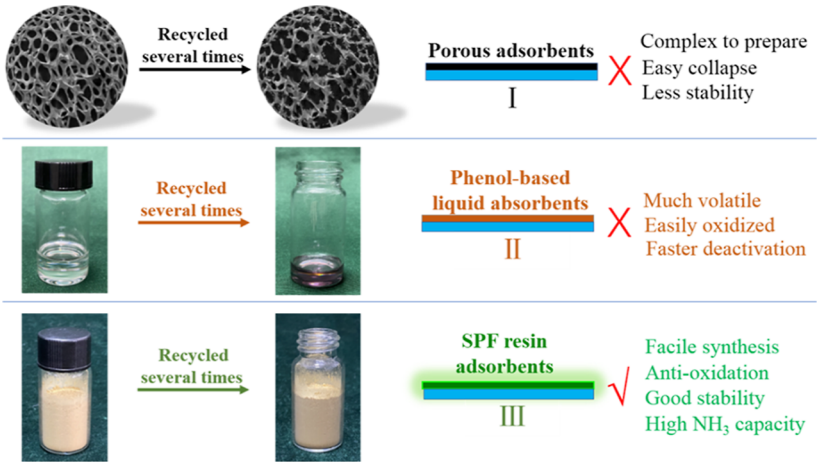

Scheme 2. Schematic Process for the Preparation of Three SPF-Based Resins

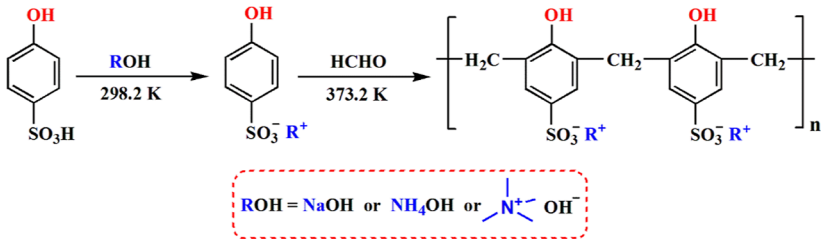

SPF resins for adsorption of NH_3, it is very promising to prepare a new SPF resin for efficient and reversible adsorption of NH_3.

Herein, three novel SPF resins were designed and prepared through the polymerization of various phenol sulfonates with formaldehyde (Scheme 2). By making use of different kinds of phenol sulfonates, the interaction of NH_3 with the hydroxyl group in phenol sulfonate can be effectively improved. As expected, the SPF resins showed highly efficient NH_3 capture and high selectivity for NH_3/H_2 and NH_3/N_2. Column breakthrough tests were further performed using 3% NH_3 in $NH_3/N_2/H_2$ mixed gas to examine the dynamic separation performance. The reusability and stability of the SPF resin were also investigated in NH_3 adsorption and desorption recycles.

EXPERIMENTAL SECTION

Materials. 4-Hydroxybenzenesulfonic acid (85%), formaldehyde (37 wt % in water), ethanol (99%), sodium hydroxide (NaOH, 96%), tetramethylammonium hydroxide (TMAOH, 25 wt % in water), and ammonia ($NH_3{\cdot}H_2O$, 25 wt % in water) were supplied from Shanghai Titan Scientific Co., Ltd. Ammonia gas (NH_3), nitrogen (N_2), and hydrogen (H_2) were purchased with a grade of 99.99 vol % from Jiangxi Huahong Special Gas Co., Ltd. All reagents and chemicals were used as received without further treatment and purification.

Preparation of SPF Resins. As shown in Scheme 2, the SPF resins were prepared by a two-step process: one is the neutralization of 4-hydroxybenzenesulfonic acid with a base (i.e., NaOH, $NH_3{\cdot}H_2O$, and TMAOH), and the other is the polymerization of phenol sulfonate with formaldehyde. In a typical run, 4-hydroxybenzenesulfonic acid (2.0 g) and NaOH (1.6 g) were dissolved in deionized water (5 mL). After stirring for 2 h, 1.6 g of formaldehyde was added to the mixture and heated at 373.2 K for 18 h under a N_2 atmosphere. After cooling, the solid product was filtered and washed with deionized water and ethanol five times. Finally, a light brown solid powder was obtained after drying at 333.2 K in vacuum for 12 h, which is designated as SPF−Na. Similarly, the resins SPF−NH_4 and SPF−TMA were prepared by the same process, except that the raw material NaOH was replaced with $NH_3{\cdot}H_2O$ and TMAOH, respectively.

Characterizations. Fourier transform infrared (FTIR) spectra were collected on a NEXUS870 FTIR spectrometer. The X-ray diffraction (XRD) pattern was recorded using a Rigaku RINT-2200 diffractometer. X-ray photoelectron spectroscopy (XPS) was performed using an AXIS SUPRA spectrometer. Thermogravimetric analysis (TGA) was performed on a PerkinElmer Diamond analyzer under a N_2 atmosphere. Field emission scanning electron microscopy (SEM) images were obtained using a HITACHI S-3400N microscope, and transmission electron microscopy (TEM) tests were performed using a JEOL JEM-2100 microscope. H_2 and N_2 sorption analyses were conducted on a Micromeritics Tristar II 3020, and the Brunauer−Emmett−Teller (BET) method was used to calculate the surface area of samples.

NH_3 Adsorption Procedure. The dual-chamber apparatus was used to measure NH_3 adsorption capacity (Figure S1, Supporting Information).[28] In a typical run, a known mass of the sample was deposited in the adsorption chamber. NH_3 in the storage chamber was introduced into the adsorption chamber. After reaching equilibrium, the adsorption data were calculated by a dual-chamber volumetric method. Three repeated operations were run for obtaining average values of NH_3 adsorption. For recycling, the NH_3-loaded SPF resin was heated at 353.2 K under vacuum for 2 h to release NH_3, and the regenerated resin was used for the next test.

https://doi.org/10.1021/acs.iecr.2c03789
Ind. Eng. Chem. Res. 2023, 62, 1542−1549

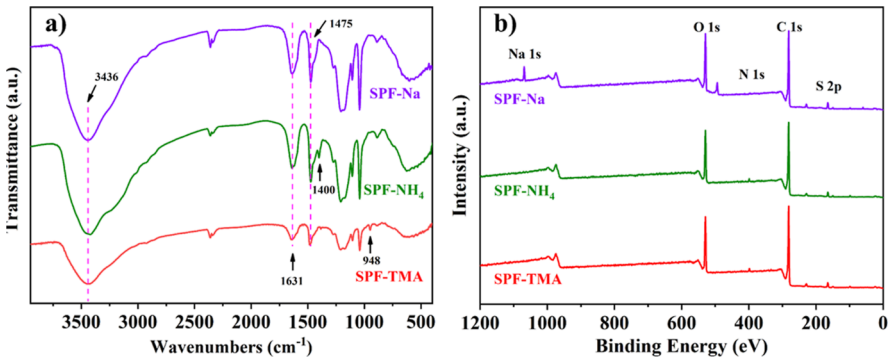

Figure 1. (a) FTIR and (b) XPS spectra of the SPF resins.

Breakthrough Tests. The breakthrough experiment of three SPF resins for NH_3 adsorption was measured on a home-made breakthrough apparatus at 298.2 K (Figure S2, Supporting Information). The detailed procedure is shown in the Supporting Information.

RESULTS AND DISCUSSION

Characterization. Figure 1a shows the FTIR spectra of the as-prepared SPF−Na, SPF−NH_4, and SPF−TMA resins. It is found that these three SPF resins displayed the typical benzene ring skeleton stretching vibration at 1475 and 1631 cm^{-1} and the O−H stretching peak in phenol at around 3436 cm^{-1}.[29−32] The characteristic peak at 1400 cm^{-1} was assigned to the group of NH_4^+ in SPF−NH_4,[11] and the peak at 948 cm^{-1} was attributed to the asymmetric C−N stretching from quaternized ammonium groups of SPF−TMA.[33] Subsequently, the results of XPS characterization confirmed the presence of N, S, C, and O elements in these three SPF resins (Figure 1b). These demonstrate that the SPF−Na, SPF−NH_4, and SPF−TMA resins were successfully prepared using the raw materials phenol sulfonate and formaldehyde. Moreover, the crystal characteristic of these SPF resins was examined. XRD patterns (Figure S3, Supporting Information) show that only a broadened peak at $2\theta = 22°$ was observed, which verifies the amorphous feature of these SPF resins.

In addition, the thermal stability of SPF resins was tested (Figure S4, Supporting Information). It is found that all three SPF resins remained largely intact when the temperature was as high as 533.2 K, suggesting their good thermal stability. The porosity feature of SPF resins was studied by N_2 sorption analysis at 77 K (Figure 2). It is indicated that all these three SPF resins exhibited very low N_2 uptake capacities and their surface area were much less than 11 $m^2 \cdot g^{-1}$. As shown in Figure 3, the SPF−Na resin showed the features of irregularity and amorphousness (Figure 3a), which is similar to the morphologies of SPF−NH_4 and SPF−TMA (Figure S5, Supporting Information). Especially, the TEM image (Figure 3b) verified the dense framework and nonporous property of the SPF-Na resin.

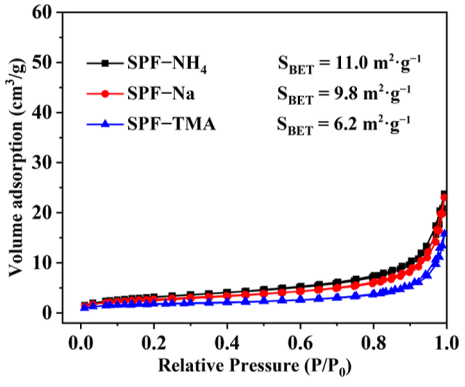

Figure 2. N_2 adsorption/desorption isotherms of the SPF resins at 77 K.

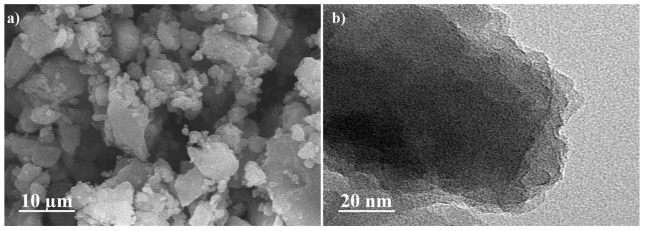

Figure 3. (a) SEM and (b) TEM images of the SPF−Na resin.

NH_3 Adsorption Performance. Figure 4a shows the NH_3 adsorption rate of the as-prepared SPF resins and common PF resin at 298.2 K and 1.0 bar. It is observed that the SPF resins exhibited much faster adsorption rates than the common PF resin. The SPF resins could quickly reach adsorption equilibrium within 3 min, while the common PF resin still could hardly reach the equilibrium even after more than 20 min with a very low capacity of 1.9 $mmol \cdot g^{-1}$. The NH_3 uptake capacities after reaching the equilibrium for the SPF resins were 4−6 times as high as that of the common PF resin. This is because the SPF resins have a sulfonate group in contrast with the common PF resin, and the electron-withdrawing sulfonate group on the benzene ring can greatly improve the interaction of the phenolic hydroxyl group with NH_3. As a result, the SPF resins showed a better NH_3 adsorption rate and resulted in a higher NH_3 uptake capacity. In addition, the SPF−NH_4 and SPF−Na resins exhibited very high NH_3 uptake capacities of 12.90 and 12.87 $mmol \cdot g^{-1}$, respectively, which are much better than that of many reported solid materials such as active carbon, zeolites, and MOFs.[34,35] However, the SPF−TMA resin exhibited a relatively low NH_3 uptake capacity of 9.83 $mmol \cdot g^{-1}$. This finding demonstrates that choosing different cations can have an effective impact on the interaction of SPF resin with NH_3. The sequence for the size of the cation is as follows: $Na^+ < NH_4^+ < TMA^+$. That is to say, the smaller cation has lower steric hindrance and facilitates the binding of the sulfonate anion with NH_3 to achieve the large NH_3 uptake capacity.

https://doi.org/10.1021/acs.iecr.2c03789
Ind. Eng. Chem. Res. 2023, 62, 1542−1549

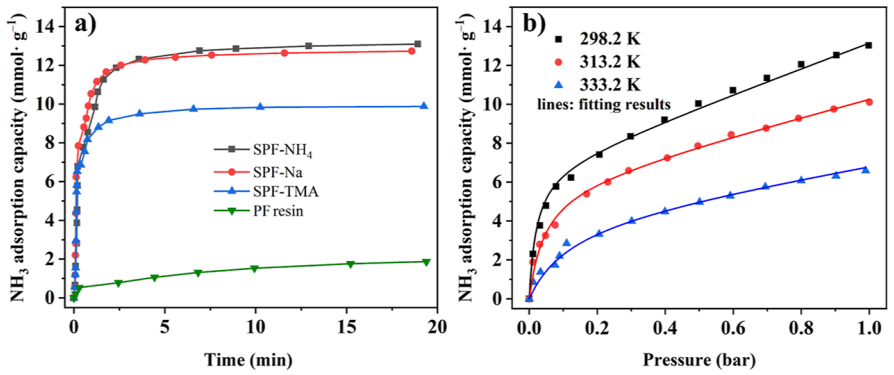

Figure 4. (a) NH_3 adsorption rate of the SPF resins and (b) NH_3 adsorption isotherms of the SPF−Na resin at different temperatures.

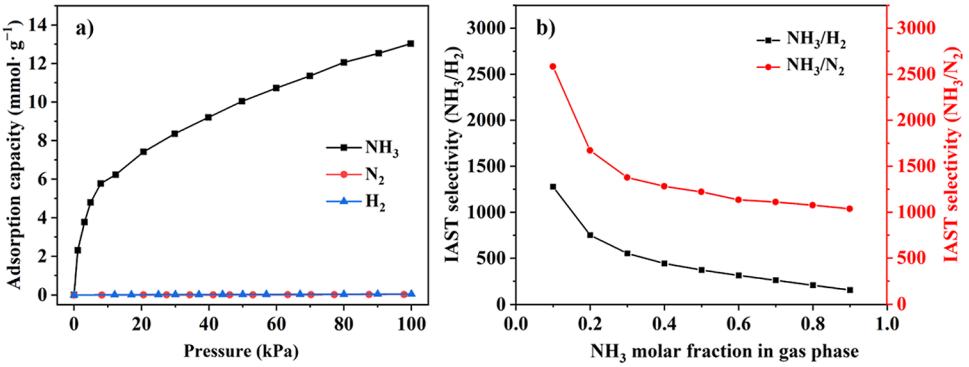

Figure 5. (a) NH_3, H_2, and N_2 adsorption on the SPF−Na resin at 298.2 K and 1.0 bar and (b) IAST selectivities to NH_3/H_2 and NH_3/N_2.

Subsequently, the effect of temperature and pressure on NH_3 adsorption by the SPF resins was examined. It is found that for these three SPF resins, all the adsorption capacities of NH_3 reduced with increasing temperature (Figures 4b and S6, Supporting Information), which follows the rule that the adsorption process is exothermic. Moreover, the NH_3 adsorption capacity could enhance linearly with the increase in NH_3 pressure from 0.2 to 1.0 bar (Figure 4b). This is to say, a high NH_3 partial pressure is favorable for the adsorption of NH_3. However, in the low pressure area of 0.01−0.2 bar, the SPF−Na resin notably had a steep increase in the NH_3 adsorption capacity (Figure 4b). For example, when the NH_3 partial pressure increased from 0.01 to 0.08 bar, the NH_3 uptakes sharply improved from 2.3 to 5.78 mmol·g^{-1}. The trend of the NH_3 adsorption on the SPF−Na resin at the low pressure obviously deviated from the ideal linear. This shows that except for physical adsorption, a chemisorption interaction would take place between NH_3 and the SPF−Na resin.

Dynamic Breakthrough Performance. Since the competitive gases (N_2 and H_2) coexist with NH_3 in the ammonia industry, it is highly important and necessary to examine the ability to selectively capture NH_3. As shown in Figure 5a, the adsorption isotherms of NH_3, H_2, and N_2 on the SPF−Na resin were investigated at 298.2 K with the pressure ranging from 0 to 1.0 bar. The NH_3 adsorption capacity was found to be as high as 12.87 mmol·g^{-1} at 1.0 bar, while it was only 0.048 and 0.02 mmol·g^{-1} for H_2 and N_2, respectively. The SPF−NH_4 and SPF−TMA resins also exhibited very low adsorption capacities of N_2 and H_2 (Figure S7, Supporting Information). The exclusion of N_2 and H_2 adsorption by these three SPF resins is mainly due to their special non-porous feature. Furthermore, the selectivities of NH_3/N_2 and NH_3/H_2 on these SPF resins were calculated based on the ideal adsorption solution theory (IAST).[36] It is indicated that all SPF resins displayed excellent NH_3/N_2 and NH_3/H_2 selectivities at 1.0 bar and 298.2 K (Figures 5b and S7, Supporting Information). For example, superior IAST selectivities for 3% NH_3/97% N_2 (5076) and 3% NH_3/97% H_2 (2619) were achieved for SPF−Na resin at 1.0 bar and 298.2 K.

To investigate the adsorption separation of the simulated mixture gas $NH_3/H_2/N_2$, a dynamic breakthrough test was performed with a gas flow rate of 30 mL·min^{-1} at 298.2 K. As shown in Figure 6, all SPF resins showed a good retention time of higher than 29 min·g^{-1} for NH_3 adsorption. Especially for the SPF−Na resin, the retention time on NH_3 could reach up to 52 min·g^{-1}. However, the breakthrough of H_2 and N_2 occurred almost instantaneously. These confirm that the SPF−

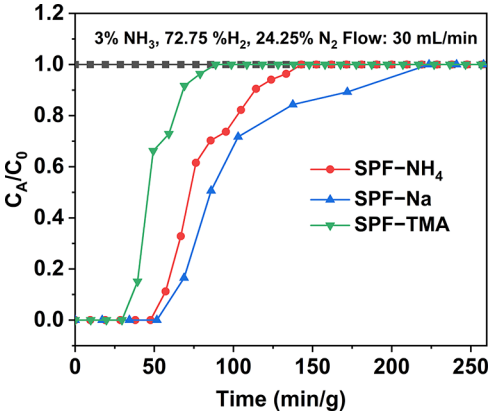

Figure 6. Experimental column breakthrough curves for 3% NH_3/72.75% H_2/24.25% N_2 separation on the SPF resins at 298.2 K.

https://doi.org/10.1021/acs.iecr.2c03789
Ind. Eng. Chem. Res. 2023, 62, 1542−1549

Na resin can selectively capture NH_3 from H_2 and N_2, indicating that the SPF−Na resin can be adopted for selective adsorption of NH_3 in an ammonia plant.

Thermodynamic Analysis. The empirical formula[37] was employed to study the chemical and physical adsorption behavior between NH_3 and the SPF−Na resin, and the total NH_3 uptake capacity (eq 1) is composed of two parts including x_R and x_H, which represent the abilities of chemical adsorption (eq 2) and physical adsorption (eq 3), respectively.

$$x = x_R + x_H = x_e \frac{KP}{1 + KP} + \frac{P}{H} \quad (1)$$

$$x_R = x_e \frac{KP}{1 + KP} \quad (2)$$

$$x_H = \frac{P}{H} \quad (3)$$

where x_e is the maximum adsorption capacity of chemical adsorption (mol·kg^{-1}), k is the adsorption equilibrium constant (kPa^{-1}), and H is the Henry constant (kPa·kg·mol^{-1}).

The fitting curves of NH_3 adsorption on the SPF−Na resin is shown in Figure 4b, and the estimated parameters are listed in Table 1. It can be seen that the curves fitted well with the experimental data with $R^2 > 0.99$. Then, the chemical and physical adsorption curves of NH_3 on the SPF−Na resin were calculated and are shown in Figure 7. It is found that the chemisorption dominated at the pressure range from 0 to 0.2 bar and the chemical adsorption capacity became flat at the pressure range from 0.2 to 1.0 bar. On the other hand, the physical adsorption capacity could enhance linearly with the increase of NH_3 partial pressure. Furthermore, the relationship between the adsorption equilibrium constant (K) and temperature (T) could be described by the following equation (eq 4)[38]

Table 1. Calculated Henry's Constant (H), Reaction Equilibrium Constants (K), and x_e for NH_3 Adsorption on the SPF−Na Resin

temperature (K)	H (kPa·kg·mol^{-1})	K (kPa^{-1})	x_e(mol·kg^{-1})	R^2
298.2	15.47	47.62	6.8210	0.996
313.2	22.22	22.52	6.0046	0.995
333.2	34.72	8.25	4.3742	0.991

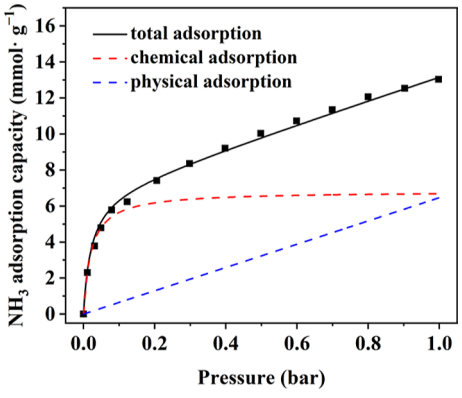

Figure 7. Total, chemical, and physical adsorption of NH_3 on the SPF−Na resin.

$$\frac{\partial \ln K}{\partial (1/T)} = -\frac{\Delta H}{R} \quad (4)$$

The linear fitting results are shown in Figure 8. The chemical adsorption enthalpy (ΔH_{chem}) is found to be −41.4 kJ·mol^{-1}.

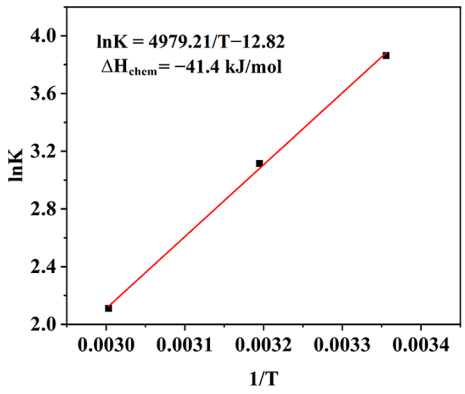

Figure 8. Linear fit of ln K and $1/T$ for NH_3 adsorption on the SPF−Na resin.

This value is much lower than the NH_3 adsorption enthalpy by the reported adsorbents in the literature.[39,40] Also, Figure S8 (Supporting Information) shows the fitting diagram of the relationship between the Henry constant (H) and temperature (T). The value of ΔH_{phy} was only −19.0 kJ/mol, further indicating the weak interaction of NH_3 physical adsorption.

Regeneration Performance. Figure 9a shows the recycling performance of the SPF−Na resin during 20 cycles. It is demonstrated that the SPF−Na resin had almost the same adsorption capacity after 20 cycles. This indicates the excellent reversibility of NH_3 adsorption on the SPF−Na resin. FTIR spectra (Figure 9b) of the SPF−Na resin were further obtained to investigate the interaction and stability change during NH_3 adsorption and desorption. After NH_3 adsorption, a new peak at 1540 cm^{-1} was observed and assigned to the bending vibration of N−H in the adsorbed NH_3. After the release of NH_3, the FTIR spectra (Figure 9b) and the XRD patterns (Figure S9, Supporting Information) of the reused SPF−Na resin were observed to remain nearly unchanged in comparison to those of the fresh SPF−Na resin after 20-cycle runs, indicating that the chemical structure of the SPF−Na resin did not change during the adsorption and desorption of NH_3. Therefore, the SPF−Na resin shows an outstanding stability and good reusability for reversible adsorption of NH_3.

Comparison of the SPF−Na Resin with Other Adsorbents in the Literature. The comparison of the SPF−Na resin with other reported porous adsorbents such as PDVB-2.0AA,[13] Mg_2(dobpdc), Ni_2(dobpdc),[17] Co_2Cl_2(BBTA),[39] COF-10,[40] NU-1000-Cl-120, NU-1000-Cl-300,[41] and NU-300[42] in terms of NH_3 adsorption capacity and reversibility is summarized and listed in Table S1 (Supporting Information). It is indicated that the adsorption capacities of NH_3 on porous adsorbents NU-1000-Cl-120, NU-1000-Cl-300, and NU-300 were obviously lower than the performance of the SPF−Na resin. In particular, porous adsorbents PDVB-2.0AA, Mg_2(dobpdc), Ni_2(dobpdc), Co_2Cl_2(BBTA), and COF-10 had a big decrease in their NH_3 adsorption capacities after a few cycles (e.g., ∼30% loss after three cycles). This is because their adsorption sites have a relatively stronger interaction for binding with NH_3 and the adsorption enthalpies

https://doi.org/10.1021/acs.iecr.2c03789
Ind. Eng. Chem. Res. 2023, 62, 1542−1549

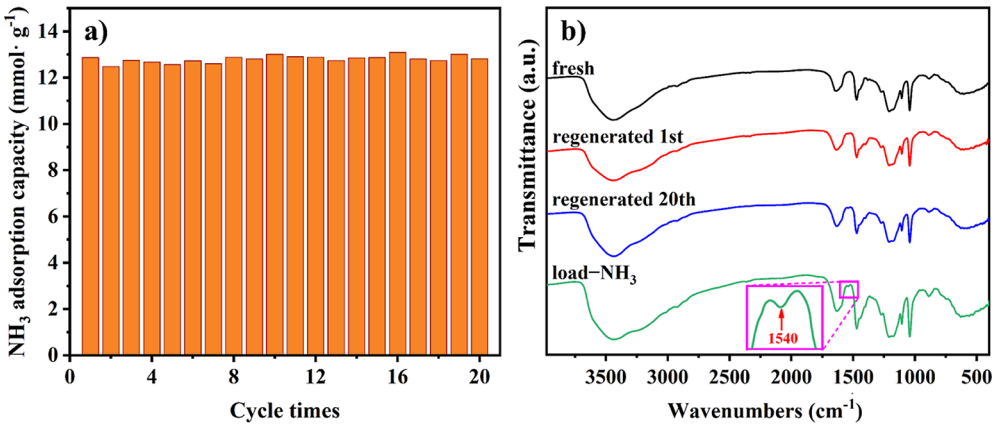

Figure 9. (a) Recycling performance of the SPF−Na resin for NH_3 adsorption and (b) FTIR spectra of SPF−Na resin before and after NH_3 adsorption.

are often higher than −50 kJ·mol^{-1}. Thus, an amount of residual NH_3 could not be desorbed and released even under high temperature and a long desorption time. By contrast, the SPF−Na resin had almost no loss NH_3 adsorption capacity during 20 cycles, and the regeneration condition was very mild. Therefore, the SPF−Na resin exhibited comprehensive performance including high NH_3 adsorption capacity, good NH_3 adsorption reversibility, and outstanding selectivity of $NH_3/H_2/N_2$.

CONCLUSIONS

In summary, three SPF resins were synthesized and employed for efficient adsorption of NH_3. The results indicated that these SPF resins with the nature of non-porosity exhibited satisfactory NH_3 adsorption capacity, good reversibility, and high selectivity with an almost exclusion of N_2 and H_2 uptakes. Particularly, the SPF−Na resin exhibited high NH_3 capacity at 298.2 K and 1.0 bar, with the amount of 12.87 mmol·g^{-1}, and the selectivities of NH_3/N_2 and NH_3/H_2 were up to 5076 and 2619, respectively. Dynamic column breakthrough tests further verified the outstanding performance of the SPF−Na resin in selective adsorption of 3% NH_3 in the mixture of $NH_3/N_2/H_2$. The 20 cycle tests also showed that the SPF−Na resin had excellent reusability and reversibility in NH_3 adsorption/desorption.

ASSOCIATED CONTENT

Supporting Information

The Supporting Information is available free of charge at https://pubs.acs.org/doi/10.1021/acs.iecr.2c03789.

Apparatus and method for the determination of NH_3 adsorption; breakthrough experiment apparatus and method; XRD patterns; TGA curves; SEM images; NH_3 adsorption isotherms; NH_3, H_2, and N_2 adsorption and IAST selectivity; physical adsorption enthalpy of NH_3 on the SPF−Na resin; XRD patterns of fresh and reused SPF−Na resin; and comparison results of the SPF−Na resin with other adsorbents in the literature (PDF)

AUTHOR INFORMATION

Corresponding Authors

Zhang-Min Li − *National Engineering Research Center for Carbohydrate Synthesis, Key Laboratory of Fluorine and Silicon for Energy Materials and Chemistry of Ministry of Education, College of Chemistry and Chemical Engineering, Jiangxi Normal University, Nanchang 330022, China*; Email: zmli@jxnu.edu.cn

Yan Zhou − *National Engineering Research Center for Carbohydrate Synthesis, Key Laboratory of Fluorine and Silicon for Energy Materials and Chemistry of Ministry of Education, College of Chemistry and Chemical Engineering, Jiangxi Normal University, Nanchang 330022, China*; orcid.org/0000-0003-0108-5061; Email: anitachow@jxnu.edu.cn

Authors

Chen Tan − *National Engineering Research Center for Carbohydrate Synthesis, Key Laboratory of Fluorine and Silicon for Energy Materials and Chemistry of Ministry of Education, College of Chemistry and Chemical Engineering, Jiangxi Normal University, Nanchang 330022, China*

Ming-Shuai Sun − *National Engineering Research Center for Carbohydrate Synthesis, Key Laboratory of Fluorine and Silicon for Energy Materials and Chemistry of Ministry of Education, College of Chemistry and Chemical Engineering, Jiangxi Normal University, Nanchang 330022, China*; orcid.org/0000-0002-5126-4159

Hua Guan − *National Engineering Research Center for Carbohydrate Synthesis, Key Laboratory of Fluorine and Silicon for Energy Materials and Chemistry of Ministry of Education, College of Chemistry and Chemical Engineering, Jiangxi Normal University, Nanchang 330022, China*

Duan-Jian Tao − *National Engineering Research Center for Carbohydrate Synthesis, Key Laboratory of Fluorine and Silicon for Energy Materials and Chemistry of Ministry of Education, College of Chemistry and Chemical Engineering, Jiangxi Normal University, Nanchang 330022, China*; orcid.org/0000-0002-8835-0341

Complete contact information is available at: https://pubs.acs.org/10.1021/acs.iecr.2c03789

Notes

The authors declare no competing financial interest.

ACKNOWLEDGMENTS

We thank the National Natural Science Foundations of China (22068013) and the Key Lab of Fluorine and Silicon for Energy Materials and Chemistry of the Ministry of Education,

Jiangxi Normal University (KFSEMC-202209) for the financial support.

REFERENCES

(1) Constable, D. J. C.; Dunn, P. J.; Hayler, J. D.; Humphrey, G. R.; Leazer, J. J. L., Jr.; Linderman, R. J.; Lorenz, K.; Manley, J.; Pearlman, B. A.; Wells, A.; Zaks, A.; Zhang, T. Y. Key green chemistry research areas—a perspective from pharmaceutical manufacturers. *Green Chem.* **2007**, *9*, 411−420.

(2) Kang, D. W.; Kang, M.; Moon, M.; Kim, H.; Eom, S.; Choe, J. H.; Lee, W. R.; Hong, C. S. PDMS-coated hypercrosslinked porous organic polymers modified via double postsynthetic acidifications for ammonia capture. *Chem. Sci.* **2018**, *9*, 6871−6877.

(3) Cheng, N. N.; Li, Z. L.; Lan, H. C.; Xu, W. L.; Huang, K. Remarkable NH_3 absorption in metal-based deep eutectic solvents by multiple coordination and hydrogen-bond interaction. *AIChE J.* **2022**, *68*, No. e17660.

(4) Zhang, J.; Yue, D.; Xia, T.; Cui, Y.; Yang, Y.; Qian, G. A luminescent metal-organic framework film fabricated on porous Al_2O_3 substrate for sensitive detecting ammonia. *Microporous Mesoporous Mater.* **2017**, *253*, 146−150.

(5) Huang, W.; Yuan, T.; Zhao, Z.; Yang, X.; Huang, W.; Zhang, Z.; Lei, Z. Coupling hydrothermal treatment with stripping technology for fast ammonia release and effective nitrogen recovery from chicken manure. *ACS Sustainable Chem. Eng.* **2016**, *4*, 3704−3711.

(6) Chen, Y.; Wang, Y.; Yang, C.; Wang, S.; Yang, J.; Li, J. Antenna-protected metal−organic squares for water/ammonia uptake with excellent stability and regenerability. *ACS Sustainable Chem. Eng.* **2017**, *5*, 5082−5089.

(7) Chen, Y.; Li, L.; Li, J.; Ouyang, K.; Yang, J. Ammonia capture and flexible transformation of M-2(INA) (M=Cu, Co, Ni, Cd) series materials. *J. Hazard. Mater.* **2016**, *306*, 340−347.

(8) Dietrich, M.; Rauch, D.; Simon, U.; Porch, A.; Moos, R. Ammonia storage studies on H-ZSM-5 zeolites by microwave cavity perturbation: correlation of dielectric properties with ammonia storage. *J. Sens. Sens. Syst.* **2015**, *4*, 263−269.

(9) Furtado, A. M. B.; Wang, Y.; Glover, T. G.; LeVan, M. D. MCM-41 impregnated with active metal sites: synthesis, characterization, and ammonia adsorption. *Microporous Mesoporous Mater.* **2011**, *142*, 730−739.

(10) Helminen, J.; Helenius, J.; Paatero, E.; Turunen, I. Adsorption equilibria of ammonia gas on inorganic and organic sorbents at 298.15 K. *J. Chem. Eng. Data* **2001**, *46*, 391−399.

(11) Takahashi, A.; Tanaka, H.; Parajuli, D.; Nakamura, T.; Minami, K.; Sugiyama, Y.; Hakuta, Y.; Ohkoshi, S.-i.; Kawamoto, T. Historical pigment exhibiting ammonia gas capture beyond standard adsorbents with adsorption sites of two kinds. *J. Am. Chem. Soc.* **2016**, *138*, 6376−6379.

(12) Yang, Y.; Faheem, M.; Wang, L.; Meng, Q.; Sha, H.; Yang, N.; Yuan, Y.; Zhu, G. Surface pore engineering of covalent organic frameworks for ammonia capture through synergistic multivariate and open metal site approaches. *ACS Cent. Sci.* **2018**, *4*, 748−754.

(13) Zhang, J.; Ma, Y.; Wu, W.; Cai, Z.; Cao, Y.; Huang, K.; Jiang, L. Carboxylic functionalized mesoporous polymers for fast, highly efficient, selective and reversible adsorption of ammonia. *Chem. Eng. J.* **2022**, *448*, 137640.

(14) Han, X.; Lu, W.; Chen, Y.; da Silva, I.; Li, J.; Lin, L.; Li, W.; Sheveleva, A. M.; Godfrey, H. G. W.; Lu, Z.; Tuna, F.; McInnes, E. J. L.; Cheng, Y.; Daemen, L. L.; MPherson, L. J. M.; Teat, S. J.; Frogley, M. D.; Rudić, S.; Manuel, P.; Ramirez-Cuesta, A. J.; Yang, S.; Schröder, M. High ammonia adsorption in MFM-300 materials: dynamics and charge transfer in host−guest binding. *J. Am. Chem. Soc.* **2021**, *143*, 3153−3161.

(15) Vikrant, K.; Kumar, V.; Kim, K.-H.; Kukkar, D. Metal−organic frameworks (MOFs): potential and challenges for capture and abatement of ammonia. *J. Mater. Chem. A* **2017**, *5*, 22877−22896.

(16) Nguyen, T. N.; Harreschou, I. M.; Lee, J.-H.; Stylianou, K. C.; Stephan, D. W. A recyclable metal−organic framework for ammonia vapour adsorption. *Chem. Commun.* **2020**, *56*, 9600−9603.

(17) Kim, D. W.; Kang, D. W.; Kang, M.; Lee, J.-H.; Choe, J. H.; Chae, Y. S.; Choi, D. S.; Yun, H.; Hong, C. S. High ammonia uptake of a metal−organic framework adsorbent in a wide pressure range. *Angew. Chem., Int. Ed.* **2020**, *59*, 22531−22536.

(18) Peterson, G. W.; Wagner, G. W.; Balboa, A.; Mahle, J.; Sewell, T.; Karwacki, C. J. Ammonia vapor removal by $Cu_3(BTC)_2$ and its characterization by MAS NMR. *J. Phys. Chem. C* **2009**, *113*, 13906−13917.

(19) Saha, D.; Deng, S. Ammonia adsorption and its effects on framework stability of MOF-5 and MOF-177. *J. Colloid Interface Sci.* **2010**, *348*, 615−620.

(20) Petit, C.; Bandosz, T. J. Enhanced adsorption of ammonia on metal-organic framework/graphite oxide composites: analysis of surface interactions. *Adv. Funct. Mater.* **2010**, *20*, 111−118.

(21) Cai, Z.; Zhang, J.; Ma, Y.; Wu, W.; Cao, Y.; Huang, K.; Jiang, L. Chelation-activated multiple-site reversible chemical absorption of ammonia in ionic liquids. *AIChE J.* **2022**, *68*, No. e17632.

(22) Cao, Y.; Zhang, J.; Ma, Y.; Wu, W.; Huang, K.; Jiang, L. Designing low-viscosity deep eutectic solvents with multiple weak-acidic groups for ammonia separation. *ACS Sustainable Chem. Eng.* **2021**, *9*, 7352−7360.

(23) Jiang, W.; Zhong, F.; Zhou, L.; Peng, H.; Fan, J.; Huang, K. Chemical dual-site capture of NH_3 by unprecedentedly low-viscosity deep eutectic solvents. *Chem. Commun.* **2020**, *56*, 2399−2402.

(24) Guan, M.; Li, H.; Chen, X.; Zhang, S. Preparation and electrochemical performance of activated carbon microspheres from recycled novolak phenol formaldehyde. *Waste Manage.* **2021**, *120*, 635−641.

(25) Farajollah Pour, M.; Khanjanzadeh, H.; Dorieh, A.; Valizadeh Kiamahalleh, M.; Doost Hoseini, K. Utilization of phenol formaldehyde/Fe_3O_4 nanocomposite as microwave preheating amplifier in laminated veneer lumber (LVL) structure. *J. Build. Eng.* **2022**, *46*, 103809.

(26) Seredych, M.; Ania, C.; Bandosz, T. J. Moisture insensitive adsorption of ammonia on resorcinol-formaldehyde resins. *J. Hazard. Mater.* **2016**, *305*, 96−104.

(27) Park, Y.; Huh, C.; Ok, J.; Cho, H. One-step synthesis and functionalization of high-salinity-tolerant magnetite nanoparticles with sulfonated phenolic resin. *Langmuir* **2019**, *35*, 8769−8775.

(28) Mao, F.; Zhou, Y.; Zhu, W.; Sang, X.; Li, Z.; Tao, D. Synthesis of guanidinium-based poly(ionic liquids) with nonporosity for highly efficient SO_2 capture from flue gas. *Ind. Eng. Chem. Res.* **2021**, *60*, 5984−5991.

(29) Li, Z.; Zhu, S.; Mao, F.; Zhou, Y.; Zhu, W.; Tao, D. CTAB-controlled synthesis of phenolic resin-based nanofiber aerogels for highly efficient and reversible SO_2 capture. *Chem. Eng. J.* **2022**, *431*, 133715.

(30) Liu, G.; Wang, Y.; Shen, C.; Ju, Z.; Yuan, D. A facile synthesis of microporous organic polymers for efficient gas storage and separation. *J. Mater. Chem. A* **2015**, *3*, 3051−3058.

(31) Zhang, T.; Li, W.; An, S.; Huang, F.; Li, X.; Liu, J.; Pei, G.; Liu, Q. Efficient transformation of corn stover to furfural using *p*-hydroxybenzenesulfonate acid-formaldehyde resin solid acid. *Bioresour. Technol.* **2018**, *264*, 261−267.

(32) Zhang, Y.; Wang, B.; Elageed, E. H. M.; Qin, L.; Ni, B.; Liu, X.; Gao, G. Swelling poly(ionic liquid)s: synthesis and application as quasi-homogeneous catalysts in the reaction of ethylene carbonate with aniline. *ACS Macro Lett.* **2016**, *5*, 435−438.

(33) Chu, J. Y.; Lee, K. H.; Kim, A. R.; Yoo, D. J. Improved electrochemical performance of composite anion exchange membranes for fuel cells through cross linking of the polymer chain with functionalized graphene oxide. *J. Membr. Sci.* **2020**, *611*, 118385.

(34) Saha, D.; Deng, S. Adsorption equilibrium and kinetics of CO_2, CH_4, N_2O, and NH_3 on ordered mesoporous carbon. *J. Colloid Interface Sci.* **2010**, *345*, 402−409.

(35) Fortier, H.; Westreich, P.; Selig, S.; Zelenietz, C.; Dahn, J. R. Ammonia, cyclohexane, nitrogen and water adsorption capacities of an activated carbon impregnated with increasing amounts of $ZnCl_2$,

https://doi.org/10.1021/acs.iecr.2c03789
Ind. Eng. Chem. Res. 2023, 62, 1542−1549

and designed to chemisorb gaseous NH_3 from an air stream. *J. Colloid Interface Sci.* **2008**, *320*, 423−435.
(36) Myers, A. L. Equation of state for adsorption of gases and their mixtures in porous materials. *Adsorption* **2003**, *9*, 9−16.
(37) Islam, M. A.; Kalam, M. A.; Khan, M. R. Reactive gas solubility in water: an empirical relation. *Ind. Eng. Chem. Res.* **2000**, *39*, 2627−2630.
(38) Zhong, F.; Peng, H.; Tao, D.; Wu, P.; Fan, J.; Huang, K. Phenol-based ternary deep eutectic solvents for highly efficient and reversible absorption of NH_3. *ACS Sustainable Chem. Eng.* **2019**, *7*, 3258−3266.
(39) Rieth, A. J.; Dincă, M. Controlled gas uptake in metal−organic frameworks with record ammonia sorption. *J. Am. Chem. Soc.* **2018**, *140*, 3461−3466.
(40) Doonan, C. J.; Tranchemontagne, D. J.; Glover, T. G.; Hunt, J. R.; Yaghi, O. M. Exceptional ammonia uptake by a covalent organic framework. *Nat. Chem.* **2010**, *2*, 235−238.
(41) Liu, J.; Chen, Z.; Wang, R.; Alayoglu, S.; Islamoglu, T.; Lee, S.-J.; Sheridan, T. R.; Chen, H.; Snurr, R. Q.; Farha, O. K.; Hupp, J. T. Zirconium metal−organic frameworks integrating chloride ions for ammonia capture and/or chemical separation. *ACS Appl. Mater. Interfaces* **2021**, *13*, 22485−22494.
(42) Chen, Y.; Zhang, X.; Ma, K.; Chen, Z.; Wang, X.; Knapp, J.; Alayoglu, S.; Wang, F.; Xia, Q.; Li, Z.; Islamoglu, T.; Farha, O. K. Zirconium-based metal−organic framework with 9-connected nodes for ammonia capture. *ACS Appl. Nano Mater.* **2019**, *2*, 6098−6102.

https://doi.org/10.1021/acs.iecr.2c03789
Ind. Eng. Chem. Res. 2023, 62, 1542−1549